Scripta Materialia 260 (2025) 116592

Contents lists available at ScienceDirect

Scripta Materialia

journal homepage: www.journals.elsevier.com/scripta-materialia

Impacts of substrate and growth temperature on the deposition and etching of c-axis oriented AlN piezoelectric thin films

Shaocheng Wu [a], Wenjiao Pei [a], Rongbin Xu [a,*], Yibo Zeng [b], Jianfang Xu [c], Baoping Zhang [a,d], Daquan Yu [a,*]

[a] School of Electronic Science and Engineering, Xiamen University, Xiamen 361005, PR China
[b] Pen-Tung Sah Institute of Micro-Nano Science and Technology, Xiamen University, Xiamen 361005, PR China
[c] College of Physical Science and Technology, Xiamen University, Xiamen 361005, PR China
[d] Institute of Nanoscience and Applications, Southern University of Science and Technology, Shenzhen 518055, PR China

ARTICLE INFO

Key words:
AlN thin film
Growth temperature
Growth substrate
Wet etching
The stability of planes

ABSTRACT

We studied the impacts of deposition substrate and temperature on the growth and wet etching behavior of AlN piezoelectric thin films. Using Mo substrate as well as optimizing temperature (450 °C), AlN films with high crystalline quality (FWHM =0.9°) and excellent piezoelectric property (d_{33}=6.3pm/V) were achieved by magnetron sputtering. Experiment results suggest that, the substrate predominantly determines the grain size and the formation of columnar structure during the initial growth stage, while the temperature mainly affects the final grain morphology. The better crystalline quality of AlN, the higher its piezoelectricity. Besides, by using TMAH solution for the wet etching of AlN films with different growth condition, it was found that the columnar grain structure is related to the chemical stability of the {10–1–2} planes, which influences the etching morphology. The etching rate shows a trend from fast to slow, and the initial rate is positively correlated with the grain size.

Nowadays, the CMOS process based on Si materials is becoming increasingly important in the manufacturing of integrated circuits [1,2]. Due to its excellent property especially the piezoelectricity and the compatibility with CMOS processes [3–5], aluminum nitride (AlN) thin films are widely used in acoustic devices [6–9] such as Bulk Acoustic Wave (BAW) and Surface Acoustic Wave (SAW) resonators. The AlN (002) crystal plane, also known as the c-axis orientation, plays a significant role in evaluating the piezoelectric property, and particularly in FBAR devices. FBAR devices fabricated by AlN with high (002) orientation exhibits larger effective coupling coefficient and Q factor. [7,8]. At present, commercialized large-sized AlN films are usually obtained by magnetron sputtering on Si substrate. However, the significant differences in lattice and thermal expansion coefficients between AlN and Si [10–12] lead to numerous defects and forming a high density of grain boundaries in AlN film epitaxially grown on Si [13], which limits its application potential in the semiconductor field. Molybdenum (Mo) has a lattice constant close to that of AlN [14,15], making it a suitable substrate for AlN epitaxy to ameliorate the mismatch. With the improvement of an AlN-interlayer, high-quality Mo film can be prepared based on Si substrate, thereby enabling the deposition of high-quality AlN piezoelectric thin films [16,17]. In addition to the substrate, the growth conditions of magnetron sputtering also affects the deposition of AlN piezoelectric thin film, especially temperature [18,19]. The growth temperature affects the kinetic energy of sputtered particles, thereby influencing the growth quality of AlN film [20]. In addition, since the growth substrate and temperature determine the quality of AlN piezoelectric thin film, they will also affect its wet etching characteristics. Wet etching typically uses acid and alkali solutions to react with AlN, such as potassium hydroxide (KOH), tetramethylammonium hydroxide (TMAH), and phosphoric acid (H_3PO_4) [21–23]. Typically, sputtering will result in the formation of N-polar AlN [24]. During wet etching of N-polar AlN, the presence of chemically stable crystallographic planes causes the etching solution to preferentially etch other planes [25–27], including the film surface defined by the (0001) plane. Ultimately, an etching morphology is defined by the planes that exhibit the slowest etching rate. Single-crystal AlN typically forms hexagonal pyramids defined by the {10–1–1} family of planes [28], while polycrystalline AlN forms round cones defined by the {10–1–2} family of planes [29,30].

* Corresponding authors.
E-mail addresses: xurongbin@xmu.edu.cn (R. Xu), yudaquan@xmu.edu.cn (D. Yu).

https://doi.org/10.1016/j.scriptamat.2025.116592
Received 18 October 2024; Received in revised form 27 January 2025; Accepted 31 January 2025
Available online 9 February 2025

Table 1
Growth parameters of AlN films of samples.

Sample name	S1	S2	S3	S4
Growth substrate	Si (100)	Si (100)	Si (100)/AlN-interlayer/Mo	Si (100)/AlN-interlayer/Mo
Growth temperature	450℃	650℃	450℃	650℃

However, the evolution of specific etching morphology and rate is rather complicated during etching stage, which hinders our understanding of wet etching mechanism of AlN film. Therefore, it is important to explore the effects of substrates and temperature on the growth and etching mechanism for high-quality AlN piezoelectric thin films, which could potentially contribute to processing of practical device application.

In this study, we investigated the growth behavior of AlN thin films under different conditions by varying the growth substrates (Si, Mo) and adjusting the growth temperatures (450℃, 650℃). These strategies have significantly enhanced our understanding of the AlN growth mechanism, enabling us to successfully deposit AlN films with high crystalline quality and superior piezoelectric property. Furthermore, the etching of AlN thin films that prepared under various substrate and temperature, was investigated at room temperature by using TMAH solution, uncovering the etching process and its underlying mechanisms.

As summarized in Table 1, 1-μm AlN thin films were deposited on 8-inch Si and Si/AlN-interlayer/Mo substrates by pulsed DC magnetron sputtering system at 450℃ and 650 ℃, respectively. Other deposition conditions are the same. Thus, the samples S1-S4 were obtained and defined. The high-quality crystalline Mo thin film was successfully deposited by using an AlN-interlayer. More detailed experimental parameters can be found in reference [16].

To better observe the etching process of AlN and explore the wet etching mechanism, a TMAH solution with a concentration of 2.38 % was used as the etching liquid to etch four samples at room temperature, enabling a slower and more controlled etching of AlN. To measure the etching rate, the AlN thin films were patterned by photoresist. The samples were etched for different durations to record the changes in thickness, thereby understanding the reaction process between AlN and the etching solution. In the wet etching process, the following chemical reactions typically occur [22]:

$$2AlN + 3H_2O \xrightarrow{N(CH_3)_4^+OH^-} Al_2O_3 + 2NH_3 \quad (1)$$

$$ScAlN + 3H_2O \xrightarrow{N(CH_3)_4^+OH^-} Al(OH)_3 + NH_3 \quad (2)$$

The morphology and roughness were characterized by Scanning Electron Microscopy (SEM, SUPRA55 SAPPHIRE, Zeiss) and Atomic Force Microscopy (AFM, Dimension FastScan, Bruker Nano Inc.). The crystal orientation and its rocking curve were measured by X-ray diffraction (XRD, X Pert PRO, PANalytical). The surface polarity distribution of AlN was tested by Piezoresponse Force Microscopy (PFM, Cypher S, Asylum Research). The etching thickness of films was obtained by step profiler (Dektak XT-A, Bruker).

To elucidate the piezoelectricity, the polarity distribution on the surface of AlN thin films were measured by PFM. As shown in Fig. 1(c-f), the PFM phase images show that all samples have mixed polarity, with yellow representing N-polarity, blue representing Al-polarity, and green representing non-polar. The predominant nonpolar part in S1 account for its minimal d_{33}. Among the remaining three samples, N-polarity is dominant, with a proportion of S3 > S2 > S1, which corresponds to the measured piezoelectric coefficient d_{33}.

To further investigated the differences in FWHM and d_{33} for four samples, the morphologies of different samples are measured by SEM, as shown in Fig. 2. AlN films grown at 450℃ (S1, S3) has distinct columnar crystals with a surface covered in spherical grains; AlN grown at 650℃ (S2, S4) does not show clear columnar crystals and has a flaky grain surface. In contrast to S4, S2 presents a columnar crystal structure in the early stages of growth. Overall, the grain size of AlN grown on Mo is larger than that of AlN grown on Si.

The differences of morphology for four samples can be explained as follows: for S1, due to the high lattice mismatch of 42.7 % between Si

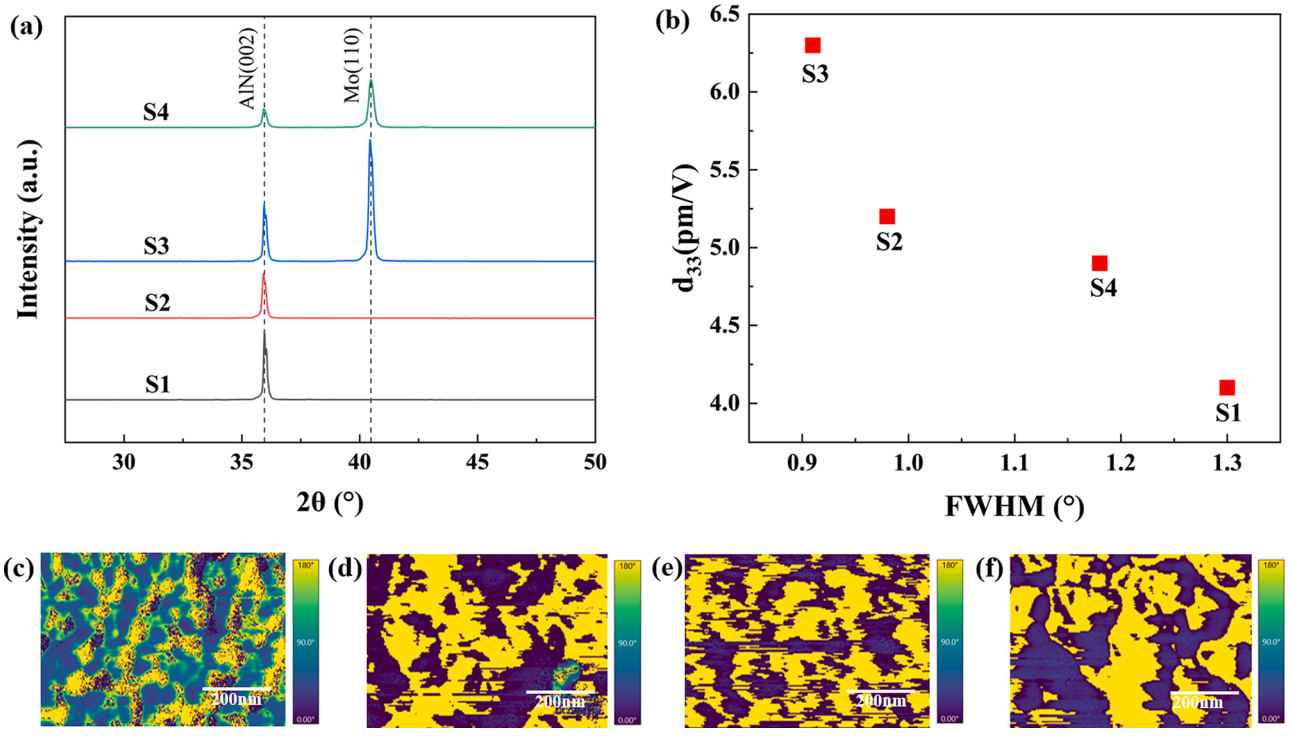

Fig. 1. (a) The XRD 2θ scan results and (b) the FWHM of XRD rocking curves and the piezoelectric coefficient d_{33} of different samples; the PFM phase images of different samples: (c) S1; (d) S2; (e) S3; (f) S4.

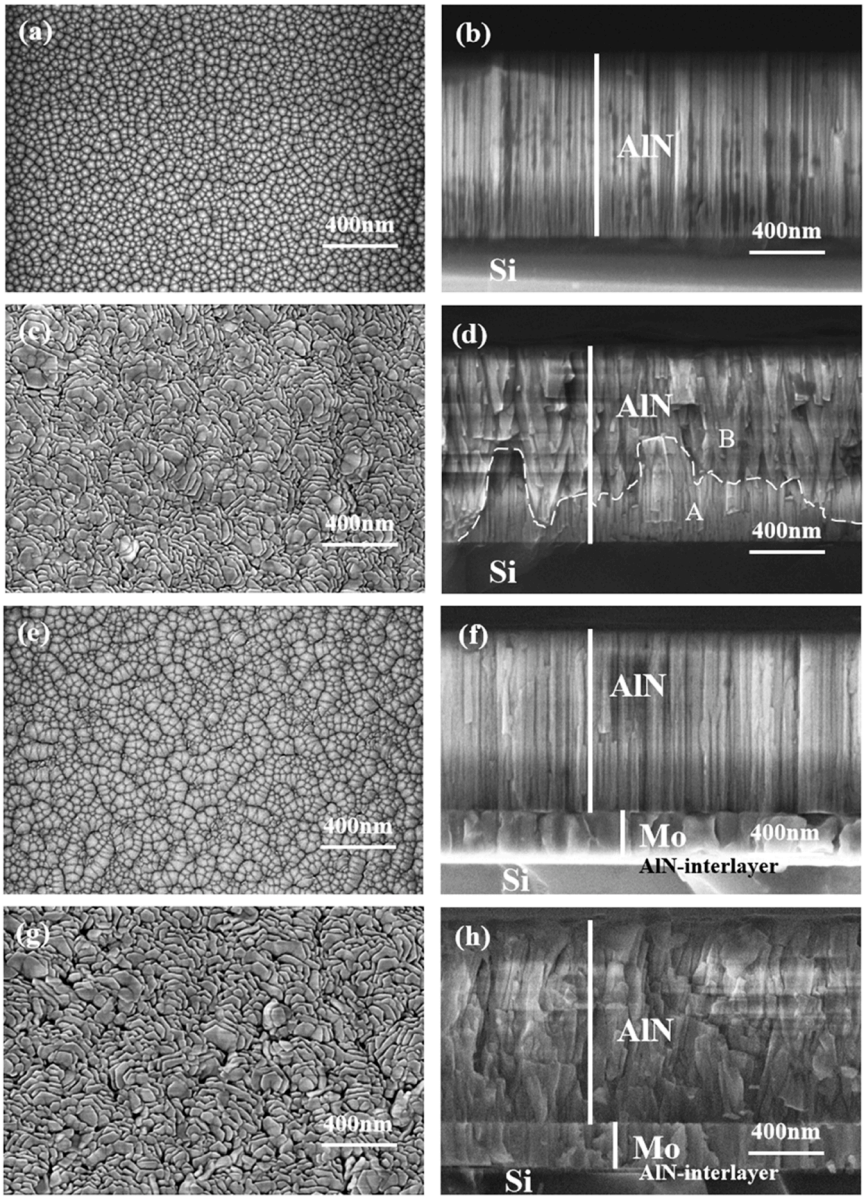

Fig. 2. SEM images of top view and cross-sectional view of different samples: (a)(b) S1; (c)(d) S2; (e)(f) S3; (g)(h) S4.

(100) and AlN (002) (the lattice mismatch calculated method is from Ref [14]), there are a large number of defects in AlN thin film after nucleation, forming a high-density grain boundary. During the growth process, the grains gradually merge and improve, forming a columnar structure. In S2, two structures (defined as Region A and B) were formed during the growth, as shown in Fig. 2(d). In Region A, Si still exerts a constraining influence on the growth of AlN in the initial stages, persisting the fine columnar crystal structure observed in S2. In the later stages, high growth temperature facilitates the coalescence and expansion of AlN grains, resulting in the increase of grain size and improved crystallographic quality in Region B. This also leads to the disappearance of columnar crystals and the appearance of flaky grains on the surface. As for S3, the lattice mismatch between Mo (110) and AlN (002) is only 1.2 %, which significantly reduces the lattice mismatch and consequently diminishes the defects such as grain boundaries. This leads to an increase in grain size and the improvement in the crystalline quality of AlN in S3. As shown in Fig. 2(e), the AlN grains exhibit a tendency to aggregate, indicating an enhancement in preferred orientation. For S4, compared with S2, the lattice mismatch between AlN and substrate is diminished, and there is no columnar crystal stage caused by substrate limitation in the early growth stage. In contrast to S3, the close lattice constant of AlN and Mo means that increasing the temperature has a minimal effect on improving the lattice mismatch between the two materials. The growth temperature primarily affects the kinetic energy of the sputtered particles. At 650 °C, the increased kinetic energy promotes grain growth and coalescence, but excessive kinetic energy may damage the film surface, leading to a deterioration in crystalline quality [31]. In summary, it can be concluded that the substrate primarily influences the grain size and columnar structure during the initial growth stage, while the growth temperature predominantly has a significant impact on the ultimate morphology of the grains.

The etching behavior of AlN thin films grown under different substrates and temperatures were investigated by using TMAH solution. To better understand the etching morphology, Fig. 3 shows the top view and 45° tilted view of S1 and S2 etched for 30 mins, and S3 and S4 etched for 10 mins. It can be seen that round cones are formed in S3 (Fig. 3(f)) and rough round cones are formed in S1 (Fig. 3(b)) and S4 (Fig. 3(h)), while a strip-like structure is formed in S2 (Fig. 3(d)).

The following gives a specific analysis of the etching process and mechanism of each sample: as shown in Fig. 4(a) (cross-sectional SEM of

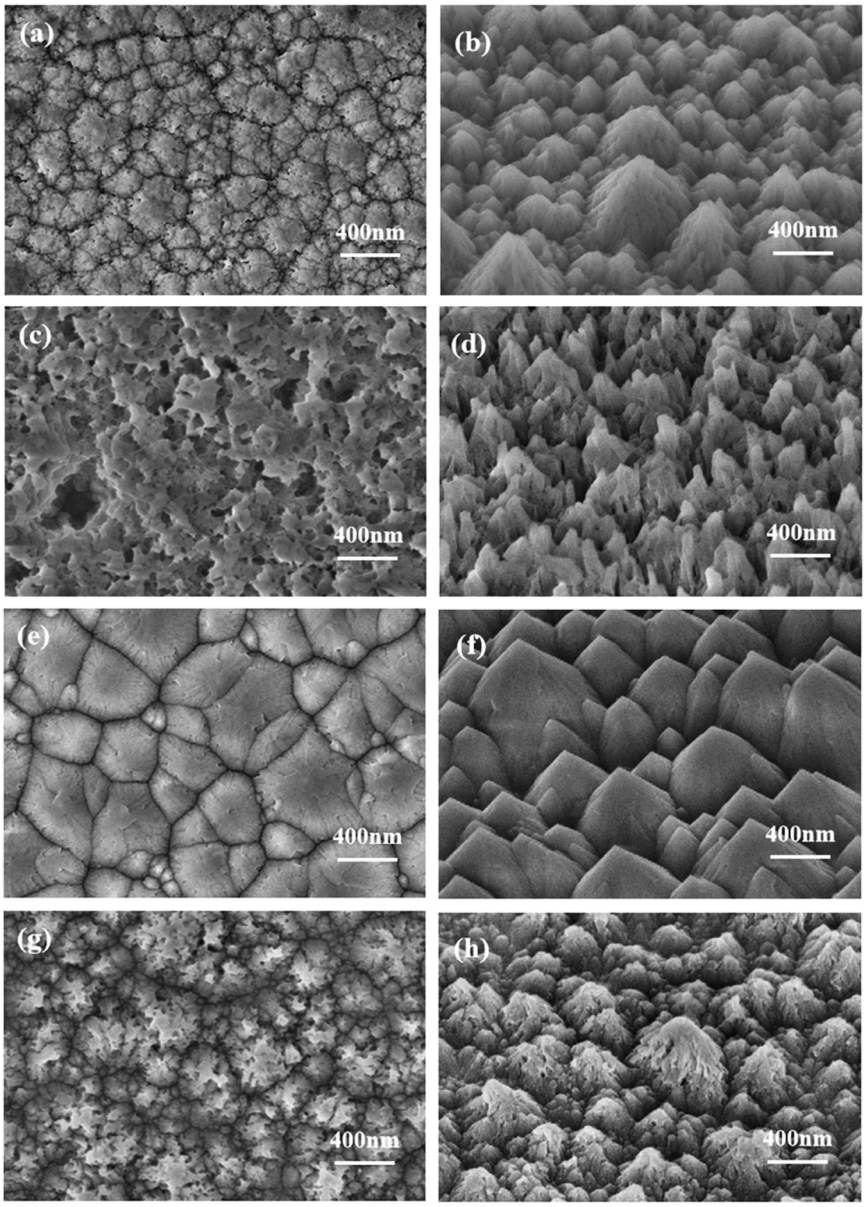

Fig. 3. SEM images of top view and 45° tilted view of different samples after etching: (a)(b) S1; (c)(d) S2; (e)(f) S3; (g)(h) S4.

S3), the surface of round cones in S3 corresponding to the {10–1–2} planes of polycrystalline AlN thin films is smooth [29,30], indicating the formation of chemically stable {10–1–2} planes. The etching solution initially etches the surface of the thin film and then proceeds to etch the grain boundaries of the columnar crystals. When etching the {10–1–2} planes, the rate of etching significantly decreases due to its enhanced chemical stability compared to other crystal planes, ultimately resulting in a conical surface morphology. S1 develops a conical structure with etching wrinkle structure after etching. This texture suggests a lower chemical stability of the {10–1–2} planes compared to S3, due to the lattice mismatch between Si and AlN. Both S1 and S3 have a columnar crystal structure, indicating that this structure is beneficial for the formation of a more stable set of {10–1–2} crystallographic planes. The relationship between the columnar structure and the planes is shown in Fig. 4(b).

The lateral grain boundary distribution in S4 shown in Fig. 2(h) is notably irregular and lacks the columnar structure, hindering the formation of stable {10–1–2} planes. Therefore, the morphology after etching (Fig. 3(h)) is conical, although the surface of cones is rough due to a large number of cracks and holes. For S2, as mentioned previously, two structures were formed during the growth as shown in Fig. 2(d), which results in two stages of the etching process as shown in Fig. 4(c-f). When etching Region B without columnar structure, there is no formation of round cones but instead of a strip-like structure, indicating the absence of {10–1–2} planes. The growth of grains in the late stage led to the emergence of other planes in Region B. Consequently, as shown in Fig. 4(c), the N-polar AlN is selectively etched away and becomes depressions, while the Al-polarity is preserved and manifests as protrusions [25,32]. When etching Region A with columnar structure, the cones is formed as shown in Fig. 4(e). This further suggests that the columnar structure facilitates the stabilization of the {10–1–2} planes, leading to an etching cone structure. This is consistent with what we previously discussed about S1 and S3.

The etching rate and etching thickness as a function of etching time are shown in Fig. 5. It can be seen that the etching rate of S1, S3, and S4 decrease continuously with the increase of etching time. This is because their etching morphology has a conical structure. Before the conical surface defined by the {10–1–2} planes are fully exposed, the part that

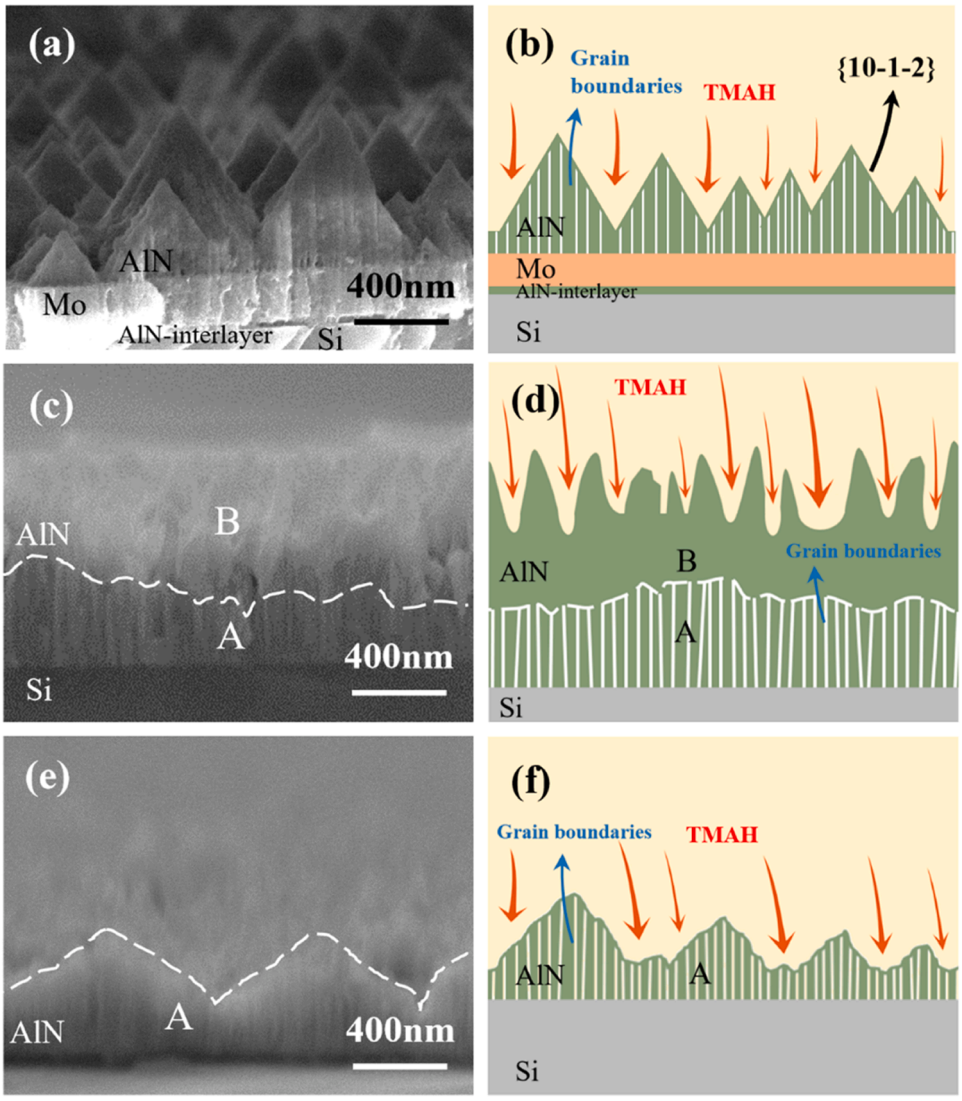

Fig. 4. (a) cross-sectional SEM image and (b) its corresponding schematic of S3 etching for 10min. Cross-sectional SEM images and their corresponding schematics of S2 under different etching time: (c) (d)10 min; (e) (f)40min.

react with the etching solution is relatively more susceptible to etch, resulting in a faster rate; when the solution reaches the planes, a conical structure is formed due to its chemical stability so the etching rate decreases.

The initial etching rate is shown as: S4 > S3 > S1. This phenomenon corresponds to the grain size on the surface of the AlN thin films. Take S1 for instance, its relatively small grain size leads to the formation of smaller cones during etching, so there is also less etching part before etching to the {10–1–2} planes. Therefore, S1 has a smaller initial etching rate compared to S3 and S4. S4 has the highest initial etching rate due to its largest grain size and poor stability of the planes. For S2, its two etching stages are also reflected in its etching rate. The first stage (0–30 min) forms a strip-like morphology with fluctuating but insignificantly changing etching rates. After 30 mins of etching, the columnar crystals formed during the initial growth exhibits a conical structure, and the etching rate gradually decreased like the other three samples.

In summary, the effects of substrate and temperature on the growth and wet etching characteristics of AlN piezoelectric thin films have been thoroughly investigated. The substrate primarily influences the grain size and columnar structure during the initial growth stage and the temperature mainly affects the final morphology of the grains. The crystalline quality of AlN has a significant impact on its piezoelectric performance: the better the crystalline quality, the higher the piezoelectric coefficient d_{33}. The mixed polarity distributed on the surface of AlN correlate with the d_{33} and the etching morphology. The columnar grain structure is related to the chemical stability of the {10–1–2} planes, and the stability can affect the integrity of the conical morphology after etching. The etching rate initially increases rapidly due to the susceptible etching planes and then decelerates as the more resistant {10–1–2} planes are exposed. The initial etching rate is positively correlated with the grain size. This work is of significant importance for AlN thin films with high quality and high piezoelectricity for their further applications.

CRediT authorship contribution statement

Shaocheng Wu: Writing – review & editing, Writing – original draft, Methodology, Investigation. **Wenjiao Pei:** Writing – review & editing, Methodology. **Rongbin Xu:** Writing – review & editing, Supervision, Methodology, Conceptualization. **Yibo Zeng:** Methodology. **Jianfang Xu:** Methodology. **Baoping Zhang:** Supervision. **Daquan Yu:** Writing – review & editing, Supervision, Resources, Funding acquisition.

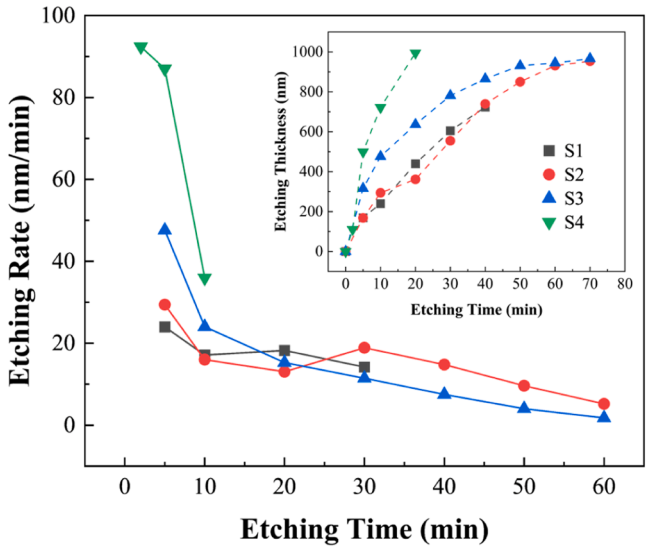

Fig. 5. Etching rate and etching thickness (the inset) as a function of etching time for different samples.

Declaration of competing interest

The authors declare that they have no known competing financial interests or personal relationships that could have appeared to influence the work reported in this paper.

Acknowledgments

This work is supported by the National Natural Science Foundation of China (grant no.U2241222).

References

[1] W. Wei, A. He, B. Yang, Z. Wang, J. Huang, D. Han, M. Ming, X. Guo, Y. Su, J. Zhang, T. Wang, Monolithic integration of embedded III-V lasers on SOI, Light. Sci. Appl. 12 (2023) 84, https://doi.org/10.1038/s41377-023-01128-z.

[2] Y. Wu, Y. Xiao, I. Navid, K. Sun, Y. Malhotra, P. Wang, D. Wang, Y. Xu, A. Pandey, M. Reddeppa, W. Shin, J. Liu, J. Min, Z. Mi, InGaN micro-light-emitting diodes monolithically grown on Si: achieving ultra-stable operation through polarization and strain engineering, Light. Sci. Appl. 11 (2022) 294, https://doi.org/10.1038/s41377-022-00985-4.

[3] D.K.T. Ng, L. Xu, Y.H. Fu, W. Chen, C.P. Ho, J.S. Goh, W.W. Chung, N. Jaafar, Q. Zhang, L.Y.T. Lee, CMOS AlN and ScAlN pyroelectric detectors with optical enhancement for detection of CO_2 and CH_4 gases, Adv. Elect. Mater. 9 (2023) 2300256, https://doi.org/10.1002/aelm.202300256.

[4] M. Wei, Y. Liu, Y. Qu, X. Gu, Y. Wang, W. Liu, Y. Cai, S. Guo, C. Sun, Development of temperature sensor based on AlN/ScAlN SAW resonators, Electronics. (Basel) 12 (2023) 3863, https://doi.org/10.3390/electronics12183863.

[5] H. Yang, J. Sun, H. Wang, H. Li, B. Yang, A review of oriented wurtzite-structure aluminum nitride films, J. Alloys. Compd. 989 (2024) 174330, https://doi.org/10.1016/j.jallcom.2024.174330.

[6] H. Wang, L. Zhang, Z. Zhou, L. Lou, Temperature performance study of SAW sensors based on AlN and AlScN, Micromachines. (Basel) 14 (2023) 1065, https://doi.org/10.3390/mi14051065.

[7] X. Yi, L. Zhao, P. Ouyang, H. Liu, T. Zhang, G. Li, High-quality film bulk acoustic resonators fabricated on AlN films grown by a new two-step method, IEEE Electron. Dev. Lett 43 (2022) 942–945, https://doi.org/10.1109/LED.2022.3164972.

[8] Y. Wang, C. Gao, C. Yang, T. Yang, Y. Liu, Y. Ma, X. Ren, Y. Cai, C. Sun, High-Q film bulk acoustic resonator with high quality AlN film based on transfer method, Phys. Scr. 99 (2024) 095926, https://doi.org/10.1088/1402-4896/ad6719.

[9] Z. Yang, F. Wang, W. Nie, X. Han, X. Guo, X. Shan, X. Lin, H. Dun, Z. Sun, Y. Xie, K. Zhang, Surface acoustic wave temperature sensor based on Pt/AlN/4 H-SiC structure for high-temperature environments, Sens. Actuat. A: Phys. 357 (2023) 114379, https://doi.org/10.1016/j.sna.2023.114379.

[10] B. Riah, J. Camus, A. Ayad, M. Rammal, R. Zernadji, N. Rouag, M.A. Djouadi, Hetero-epitaxial growth of AlN deposited by DC magnetron sputtering on Si(111) using a AlN buffer layer, Coatings 11 (2021) 1063, https://doi.org/10.3390/coatings11091063.

[11] V.N. Bessolov, E.V. Gushchina, E.V. Konenkova, S.D. Konenkov, T.V. L'vova, V. N. Panteleev, M.P. Shcheglov, Synthesis of hexagonal AlN and GaN layers on a Si (100) substrate by chloride vapor-phase epitaxy, Tech. Phys. 64 (2019) 531–534, https://doi.org/10.1134/S1063784219040054.

[12] I.-S. Shin, J. Kim, D. Lee, D. Kim, Y. Park, E. Yoon, Epitaxial growth of single-crystalline AlN layer on Si(111) by DC magnetron sputtering at room temperature, Jpn. J. Appl. Phys. 57 (2018) 060306, https://doi.org/10.7567/JJAP.57.060306.

[13] Z.Q. Yao, Q. Ye, Y.Q. Li, Y.S. Zou, W.J. Zhang, S.T. Lee, Microstructure analysis of c-axis oriented aluminum nitride thin films by high-resolution transmission electron microscopy, Appl. Phys. Lett. 90 (2007) 121907, https://doi.org/10.1063/1.2715173.

[14] S. Imran, J. Yuan, G. Yin, Y. Ma, S. He, Influence of metal electrodes on *c* -axis orientation of AlN thin films deposited by DC magnetron sputtering, Surf. Interf. Anal. 49 (2017) 885–891, https://doi.org/10.1002/sia.6237.

[15] J. Kim, Y. Kim, S. Hong, Structural analysis of Mo thin films on sapphire substrates for epitaxial growth of AlN, Micromachines. (Basel) 14 (2023) 966, https://doi.org/10.3390/mi14050966.

[16] S. Wu, R. Xu, B. Guo, Y. Ma, D. Yu, Influence of growth parameters and systematical analysis on 8-inch piezoelectric AlN thin films by magnetron sputtering, Mater. Sci. Semicond. Process. 169 (2024) 107895, https://doi.org/10.1016/j.mssp.2023.107895.

[17] Y. Zou, C. Gao, J. Zhou, Y. Liu, Q. Xu, Y. Qu, W. Liu, J.B.W. Soon, Y. Cai, C. Sun, Aluminum scandium nitride thin-film bulk acoustic resonators for 5G wideband applications, Microsyst. Nanoeng. 8 (2022) 124, https://doi.org/10.1038/s41378-022-00457-0.

[18] A. Iqbal, G. Walker, L. Hold, A. Fernandes, A. Iacopi, F. Mohd-Yasin, Pulsed DC sputtering of highly *c* -axis AlN film on top of Si (111) substrate, Physica Status Solidi (b) 258 (2021) 2000549, https://doi.org/10.1002/pssb.202000549.

[19] S.S. Chauhan, M.M. Joglekar, S.K. Manhas, Influence of process parameters and formation of highly c-axis oriented AlN thin films on Mo by reactive sputtering, J. Elec. Mater. 47 (2018) 7520–7530, https://doi.org/10.1007/s11664-018-6695-6.

[20] A. Iqbal, G. Walker, L. Hold, A. Fernandes, P. Tanner, A. Iacopi, F. Mohd-Yasin, The sputtering of AlN films on top of on- and off-axis 3C-SiC (111)/Si (111) substrates at various substrate temperatures, J. Mater Sci: Mater Electron 29 (2018) 2434–2446, https://doi.org/10.1007/s10854-017-8163-0.

[21] Z. Tang, G. Esteves, J. Zheng, R.H. Olsson, Vertical and lateral etch survey of ferroelectric AlN/Al1−xScxN in aqueous KOH solutions, Micromachines. (Basel) 13 (2022) 1066, https://doi.org/10.3390/mi13071066.

[22] A.S.M.Z. Shifat, I. Stricklin, R.K. Chityala, A. Aryal, G. Esteves, A. Siddiqui, T. Busani, Vertical etching of scandium aluminum nitride thin films using TMAH solution, Nanomaterials 13 (2023) 274, https://doi.org/10.3390/nano13020274.

[23] C. Stoeckel, C. Kaufmann, R. Hahn, R. Schulze, D. Billep, T. Gessner, Pulsed DC magnetron sputtered piezoelectric thin film aluminum nitride – Technology and piezoelectric properties, J. Appl. Phys. 116 (2014) 034102, https://doi.org/10.1063/1.4887799.

[24] W. Guo, H. Xu, L. Chen, H. Yu, J. Jiang, M. Sheikhi, L. Li, Y. Dai, M. Cui, H. Sun, J. Ye, Polarity control and fabrication of lateral polarity structures of III-nitride thin films and devices: progress and prospects, J. Phys. D: Appl. Phys. 53 (2020) 483002, https://doi.org/10.1088/1361-6463/abaf7b.

[25] E. Wistrela, M. Schneider, A. Bittner, U. Schmid, Impact of the substrate dependent polarity distribution in c-axis oriented AlN thin films on the etching behaviour and the piezoelectric properties, Microsyst. Technol. 22 (2016) 1691–1700, https://doi.org/10.1007/s00542-015-2799-6.

[26] S.M. Tanner, V.V. Felmetsger, Microstructure and chemical wet etching characteristics of AlN films deposited by ac reactive magnetron sputtering, J. Vacuum Sci. Technol. A 28 (2010) 69–76, https://doi.org/10.1116/1.3268620.

[27] W. Guo, R. Kirste, I. Bryan, Z. Bryan, L. Hussey, P. Reddy, J. Tweedie, R. Collazo, Z. Sitar, KOH based selective wet chemical etching of AlN, AlxGa1−xN, and GaN crystals: a way towards substrate removal in deep ultraviolet-light emitting diode, Appl. Phys. Lett. 106 (2015) 082110, https://doi.org/10.1063/1.4913705.

[28] D. Zhuang, J.H. Edgar, L. Liu, B. Liu, L. Walker, Wet chemical etching of AlN single crystals, MRS Internet J. Nitride Semicond. Res. 7 (2002) e4, https://doi.org/10.1557/S1092578300000302.

[29] S. Marauska, V. Hrkac, T. Dankwort, R. Jahns, H.J. Quenzer, R. Knöchel, L. Kienle, B. Wagner, Sputtered thin film piezoelectric aluminum nitride as a functional MEMS material, Microsyst. Technol. 18 (2012) 787–795, https://doi.org/10.1007/s00542-012-1493-1.

[30] K. Airola, S. Mertin, J. Likonen, E. Hartikainen, K. Mizohata, J. Dekker, A. Thanniyil Sebastian, T. Pensala, High-fidelity patterning of AlN and ScAlN thin films with wet chemical etching, Materialia (Oxf) 22 (2022) 101403, https://doi.org/10.1016/j.mtla.2022.101403.

[31] H. Jin, B. Feng, S. Dong, C. Zhou, J. Zhou, Y. Yang, T. Ren, J. Luo, D. Wang, Influence of substrate temperature on structural properties and deposition rate of AlN thin film deposited by reactive magnetron sputtering, J. Elec. Mater. 41 (2012) 1948–1954, https://doi.org/10.1007/s11664-012-1999-4.

[32] E. Milyutin, S. Harada, D. Martin, J.F. Carlin, N. Grandjean, V. Savu, O. Vaszquez-Mena, J. Brugger, P. Muralt, Sputtering of (001)AlN thin films: control of polarity by a seed layer, J. Vacuum Sci. Technol. B, Nanotechnol. Microelectr. 28 (2010) L61–L63, https://doi.org/10.1116/1.3501117.